CDF/PUB/BOTTOM/PUBLIC/10900

Observation of the bottom baryon resonance state Λ_b^{*0} with CDF II Detector

The CDF Collaboration[1]

[1] *URL http://www-cdf.fnal.gov*

(Dated: July 23, 2012)

Using data from $p\bar{p}$ collisions at $\sqrt{s} = 1.96\,\text{TeV}$ recorded by the CDF II detector at the Fermilab Tevatron, we present an observation of the excited resonance state Λ_b^{*0} in its fully reconstructed decay mode to $\Lambda_b^0\pi^-\pi^+$ where $\Lambda_b^0 \to \Lambda_c^+\pi^-$ with $\Lambda_c^+ \to pK^-\pi^+$. The mass of the observed state is found to be $5919.5 \pm 0.35\,(\text{stat}) \pm 1.72\,(\text{syst})$. The local significance of the observed signal is 4.6σ while the significance of the signal for the search region is 3.5σ. The analysis is based on a data sample corresponding to an integrated luminosity of $9.6\,\text{fb}^{-1}$ collected by an online event selection based on tracks displaced from the $p\bar{p}$ interaction point.

TABLE I: Theoretical Predictions for Λ_b^{*0} Masses. The Q-value is defined as $Q = M(\Lambda_b^{*0}) - M(\Lambda_b^0) - 2\cdot m(\pi^\pm)$ for the hadronic decay mode of interest, $\Lambda_b^{*0} \to \Lambda_b^0\pi^+\pi^-$. The predictions by Chow *et al.* are made for the spin averaged state.

Reference	$M(\Lambda_b^0)$, MeV/c^2	$M(\Lambda_b^{*0}, \frac{1}{2}^-)$, MeV/$c^2$	Q, MeV/c^2	$M(\Lambda_b^{*0}, \frac{3}{2}^-)$, MeV/$c^2$	Q, MeV/c^2
Capstick [5]	5585	5912	47	5920	55
Karliner [6]	5619.7,CDF	5929 ± 2	29	5940 ± 2	40
Roberts [7]	5612	5939	47	5941	49
Garcilazo [11]	5625	5890	-15	5890	-15
Faustov [8]	5622	5930	28	5947	45
Zhang [12]	5690 ± 130	5850 ± 150	-120 ± 198	5900 ± 160	-70 ± 206
Baccouche [10]	5619.7,CDF	5920	20	5920	20

I. INTRODUCTION

Baryons with a heavy quark Q can be viewed as the useful laboratory of quantum chromodynamics (QCD) in its confinement domain. The heavy quark in the baryon can serve as a probe of confinement that allows the study of nonperturbative QCD in a different regime from that of the light baryons.

The models approaching the heavy hadrons in a framework of heavy quark effective theories (HQET) [1] treat the heavy baryons as a system of a heavy quark Q considered as a static color source with mass $m_Q \gg \Lambda_{\rm QCD}$ and of a light diquark qq with a gluon field [2]. As the spin S_{qq} of a light diquark and the spin S_Q of a heavy quark are decoupled in HQET, heavy baryons can be described by the quantum numbers S_Q, m_Q, S_{qq}, m_{qq}. The total spins of the S-wave (no orbital excitation) baryon multiplets can be expressed as the sum $\vec{J} = \vec{S_Q} + \vec{S}_{qq}$. Then the singlet Λ_b^0 baryon, with quark content $b[ud]$ according to HQET, has spin of the heavy quark $S_b^P = \frac{1}{2}^+$ and isospin $I = 0$. Its flavor antisymmetric $[ud]$ diquark has spin $S_{[ud]}^P = 0^+$ [3]. Under these conditions the b quark and the $[ud]$ diquark make the lowest-lying singlet ground state $J^P = \frac{1}{2}^+$. The partner of the Λ_b^0 baryon in the charm quark sector is the Λ_c^+ baryon.

Once the $[ud]$ diquark acquires an orbital excitation with $L = 1$ relative to the heavy quark b, the two excited states Λ_b^{*0} emerge with the same quark content as a singlet Λ_b^0, with isospin $I = 0$ but with a total spin $J^P = \frac{1}{2}^-$ and $J^P = \frac{3}{2}^-$ [3]. These isoscalar states are the lowest-lying P-wave states that can decay to the singlet Λ_b^0 via strong processes involving an emission of a pair of soft pions – given the parity P is conserved and provided sufficient phase space is available. Both Λ_b^{*0} particles are classified as bottom baryon resonant states. The partners of the Λ_b^{*0} states [4] in the charm quark sector are $\Lambda_c(2595)^+$ and $\Lambda_c(2625)^+$ baryons.

Some recent theoretical predictions on masses of excited heavy baryons Λ_b^{*0} are shown in Table I. One of the early calculations [5] uses an outdated mass for Λ_b^0 which is too low and biases the mass difference predictions. Karliner *et al.* [6] consider the excitations Λ_Q^* with $J^P = \frac{1}{2}^-$ and $J^P = \frac{3}{2}^-$ where a P-wave ($L = 1$) isospin-0 ($I = 0$) and spinless ($S_{qq}^P = 0^+$) diquark is coupled to the heavy quark, $S_Q^P = \frac{1}{2}^+$. Under this assumption, the difference between the spin averaged mass $M(\Lambda_Q^*)$ and the ground state mass $M(\Lambda_Q)$ is only the orbital excitation energy of the diquark. Roberts *et al.* [7] use a non-relativistic quark model with heavy baryon quark states configured according to HQET to predict the mass spectrum. The HQET calculations applied to a relativistic quark model are available in Ref. [8]. The mass spectra of single heavy quark baryons calculated with HQET in combined expansions in $1/m_Q$ and $1/N_c$, with N_c defined as a number of colors, are presented in Ref. [9]. The similar method is further applied by [10] to charm Λ_c^+ and bottom Λ_b^0 baryons and their excitations.The model predicts the mass for the spin averaged orbitally excited Λ_b^{*0} state, $M(\overline{\Lambda_b^{*0}}) \approx M(\Lambda_b^0) + 300\,\text{MeV} \approx 5920\,\text{MeV}$. Some of theoretical predictions [11, 12] for Λ_b^{*0} masses are below the hadronic decay mode threshold allowing only radiative decays for excited Λ_b^{*0} resonances. Recent lattice nonrelativistic QCD calculations [13] for bottom baryons [14–16] are quite successful though the calculations for the heavy-quark excited baryon states have not been complete.

The description of strong decays of baryon resonances is a difficult theoretical task [17]. Only few calculations [3, 16, 18, 19] for the $\Sigma_b^{(*)}$ states are available now, while the problems with the calculations for three-body decay modes of excited Λ_b^{*0} states still need to be tackled.

The first result on bottom baryon resonances was obtained by CDF with the observation of the $\Sigma_b^{(*)}$ states in $\Lambda_b^0\pi^\pm$ decay modes [20]. Recently CDF has confirmed its first observation presenting the measurements of the masses and widths of the $\Sigma_b^{(*)\pm}$ baryons [21].

LHCb (CERN) has reported the first observation of two narrow structures in an invariant mass spectrum of $\Lambda_b^0\pi^+\pi^-$ at 5912 MeV/c^2 and 5920 MeV/c^2 [22]. The structures are interpreted as the orbitally-excited $\Lambda_b^{*0}(5912)$ and $\Lambda_b^{*0}(5920)$ bottom baryon resonances.

Using a complete data sample of 9.6 fb^{-1} collected with CDF detector, we undertake a search for the resonant states produced at Tevatron and decaying in the same mode, $\Lambda_b^0\pi^+\pi^-$. The confirmation of the LHCb result that we report here stands as a second observation of Λ_b^{*0} resonance state.

Section II provides a brief description of the CDF II detector, the online event selection for this analysis, and the detector simulation. In Sec. III the data selection, analysis requirements, and reconstruction of the signal candidates are described. Section IV discusses the fit model of the final spectra and summarizes the fit results. The systematic uncertainties are discussed in Sec. V. We present a summary of the measurements and conclusions in Sec. VI.

II. THE CDF II DETECTOR AND SIMULATION

The component of the CDF II detector [23] most relevant to this analysis is the charged particle tracking system. The tracking system operates in a uniform axial magnetic field of 1.4 T generated by a superconducting solenoidal magnet. The inner tracking system comprises three silicon detectors: layer 00 (L00), the silicon vertex detector (SVX II) and the intermediate silicon layers (ISL) [24]. A large open cell cylindrical drift chamber, the central outer tracker (COT) [25], completes the CDF detector tracking system.

The trajectories of tracks reconstructed in the COT are extrapolated into the SVX II detector, and the tracks are refit with additional silicon hits consistent with the track extrapolation. The two additional layers of the ISL help to link tracks in the COT to hits in the SVX II. The combined track transverse momentum resolution is $\sigma(p_{\rm T})/p_{\rm T} \simeq 0.07\%\, p_{\rm T}\,[\,{\rm GeV}/c]^{-1}$ [26].

The analysis presented here is based on events recorded with a three-tiered trigger system configured to collect large data samples of heavy hadrons decaying through multibody hadronic channels. We refer to this as the displaced two-track trigger. At level 1, the trigger requires two tracks in the COT with $p_{\rm T} > 2.0\,{\rm GeV}/c$ for each track [27]. The level 2 silicon vertex trigger (SVT) [28] associates the track pair found at level 1 with hits in the SVX II detector. The SVT repeats the level 1 $p_{\rm T}$ criteria and limits the opening angle between the tracks to $2^\circ < |\Delta\phi| < 90^\circ$. The SVT system has an excellent resolution of 35 μm (or 50 μm when convoluted with a contribution from the beamspot) provided by SVX II. A requirement imposed by the SVT on the transverse impact parameter of each track to be $0.12 < d_0 < 1$ mm makes an effective selection of long-lived heavy-flavor particles. Finally, the distance in the transverse plane between the beam axis and the intersection point of the two tracks projected onto their total transverse momentum is required to be $L_{xy} > 200\,\mu$m. The level 3 software trigger uses a full reconstruction of the event with all detector information and confirms the criteria applied at level 2. The trigger criteria applied to the d_0 of each track in the pair and to L_{xy} preferentially select decays of long-lived heavy hadrons over prompt background, ensuring that the data sample is enriched with b hadrons.

The mass resolution on the Λ_b^{*0} resonances is predicted with a Monte Carlo simulation that generates b quarks according to a next-to-leading order calculation [29] and produces events containing final state hadrons by simulating b quark fragmentation [30]. In the Monte-Carlo simulations, the Λ_b^{*0} is assigned the mass value of 5920.0 MeV/c^2 [10]. Final state decay processes are simulated with the EVTGEN [31] program, and all simulated b hadrons are produced without polarization. The generated events are input to the detector and trigger simulation based on GEANT3 [32] and processed through the same reconstruction and analysis algorithms as are used on the data.

III. DATA SAMPLE AND EVENT SELECTION

This analysis is based on a complete CDF dataset equivalent to 9.6 fb^{-1} of $p\overline{p}$ collisions collected with the displaced two-track trigger between March 2002 and December 2011. We search for Λ_b^{*0} states in the exclusive strong decay mode $\Lambda_b^{*0} \to \Lambda_b^0\pi_s^-\pi_s^+$, where the pair of low momentum pions $\pi_s^-\,\pi_s^+$ are produced near the kinematic threshold [33]. The Λ_b^0 decays to $\Lambda_c^+\pi_b^-$ with a pion π_b^- produced in the weak decay. This is followed by the weak decay $\Lambda_c^+ \to pK^-\pi^+$.

To reconstruct the parent baryons, the tracks of charged particles are combined in a kinematic fit to form candidates. No particle identification is used in this analysis.

A. Reconstruction of the Λ_b^0 candidates

The analysis begins with reconstruction of the $\Lambda_c^+ \to pK^-\pi^+$ decay by fitting three tracks to a common vertex. The invariant mass of the Λ_c^+ candidate is required to be within ± 18 MeV/c^2 of the world-average Λ_c^+ mass [34]. The

TABLE II: Analysis requirements for $\Lambda_b^0 \to \Lambda_c^+\pi_b^-$ reconstruction. The quantity $ct(\Lambda_c^+ \leftarrow \Lambda_b^0)$ is defined analogously to $ct(\Lambda_b^0)$ as the Λ_c^+ proper time where $L_{xy}(\Lambda_c^+)$ is calculated with respect to the Λ_b^0 vertex.

Quantity	Requirement
$ct(\Lambda_b^0)$	> 200 μm
$ct(\Lambda_b^0)/\sigma_{ct}$	> 6.0
$d_0(\Lambda_b^0)$	< 80 μm
$ct(\Lambda_c^+ \leftarrow \Lambda_b^0)$	> -100 μm
$p_{\rm T}(\pi_b^-)$	> 1.0 GeV/c
$p_{\rm T}(\Lambda_b^0)$	> 9.0 GeV/c
Prob(χ^2_{3D}) of Λ_b^0 vertex fit	$> 0.01\%$

momentum vector of the Λ_c^+ candidate is then extrapolated to intersect with a fourth track that is assumed to be the pion, to form the $\Lambda_b^0 \to \Lambda_c^+\pi_b^-$ candidate. The Λ_b^0 vertex is subjected to a three-dimensional kinematic fit with the Λ_c^+ candidate mass constrained to its world-average value [34]. The probability of the constrained Λ_b^0 vertex fit must exceed 0.01%. Standard quality requirements are applied to each track, and only tracks with $p_{\rm T} > 400\,{\rm MeV}/c$ are used. All tracks are refit using pion, kaon and proton mass hypotheses to properly correct for the differences in multiple scattering and ionization energy loss. The proton from the Λ_c^+ candidate and at least one of the remaining K^-, π^+ and π_b^- track candidates both must fulfill the trigger requirements.

To suppress prompt backgrounds from the primary interaction, the decay vertex of the Λ_b^0 is required to be distinct from the primary vertex. To achieve this, cuts on a proper lifetime $ct(\Lambda_b^0)$ and its significance $ct(\Lambda_b^0)/\sigma_{ct}$ are applied. We define the proper lifetime as

$$ct(\Lambda_b^0) = L_{xy}\,\frac{M(\Lambda_b^0)\,c}{p_{\rm T}}\ .$$

We use a primary vertex determined event-by-event when computing this vertex displacement.

We require the Λ_c^+ vertex to be associated with a Λ_b^0 decay by applying cut on a proper lifetime $ct(\Lambda_c^+)$ where the corresponding quantity $L_{xy}(\Lambda_c^+)$ is calculated with respect to the Λ_b^0 vertex. The requirement $ct(\Lambda_c^+) > -100$ μm reduces contributions from Λ_c^+ baryons directly produced in $p\overline{p}$ interaction and from random combination of tracks faking Λ_c^+ candidates which may have negative $ct(\Lambda_c^+)$ values.

To reduce combinatorial background and contributions from partially reconstructed decays, we ask Λ_b^0 candidates to point to the primary vertex by requiring the impact parameter $d_0(\Lambda_b^0)$ not to exceed 80 μm.

The Λ_b^0 candidate must have $p_{\rm T}(\Lambda_b^0)$ greater than $9.0\,{\rm GeV}/c$ to get the slow pions of Λ_b^{*0} decay within the kinematic acceptance of the track reconstruction. Table II summarizes the resulting Λ_b^0 analysis requirements.

Figure 1 shows a prominent Λ_b^0 signal in the $\Lambda_c^+\pi_b^-$ invariant mass distribution, reconstructed using the criteria shown in Table II. A binned maximum-likelihood fit finds a signal of approximately 15 400 candidates at the expected Λ_b^0 mass, with a signal to background ratio around 1.1. The fit model describing the invariant mass distribution comprises the Gaussian $\Lambda_b^0 \to \Lambda_c^+\pi_b^-$ signal on top of a background shaped by several contributions. Random four-track combinations dominating the right sideband are modeled with an exponentially decreasing function. Coherent sources populate the left sideband and leak under the signal. These include reconstructed B mesons that pass the $\Lambda_b^0 \to \Lambda_c^+\pi_b^-$ selection criteria, partially reconstructed Λ_b^0 decays, and fully reconstructed Λ_b^0 decays other than $\Lambda_c^+\pi_b^-$ (*e.g.* $\Lambda_b^0 \to \Lambda_c^+K^-$). Shapes representing the physical background sources are derived from Monte Carlo simulations. Their normalizations are constrained to branching ratios that are either measured (for B meson decays, reconstructed within the same $\Lambda_c^+\pi_b^-$ sample) or theoretically predicted (for Λ_b^0 decays) [20, 35].

B. Reconstruction of Λ_b^{*0} candidates

To reconstruct the $\Lambda_b^{*0} \to \Lambda_b^0\pi_s^-\pi_s^+$ candidates, each $\Lambda_c^+\pi_b^-$ candidate with an invariant mass within the Λ_b^0 signal region, $5.561 - 5.677$ GeV/c^2, is combined with a pair of the oppositely charged tracks. The Λ_b^0 mass range covers ± 3 standard deviations as determined by a fit to the signal peak of Fig. 1. To increase the efficiency for reconstructing Λ_b^{*0} decays near the kinematic threshold, the quality criteria applied to soft pion tracks are loosened in comparison with tracks used for the Λ_b^0 candidates. The basic COT and SVX II hit requirements are imposed on $\pi_s^\pm$ tracks, and only tracks with $p_{\rm T} > 200\,{\rm MeV}/c$ that having hits in both trackers and with a valid track fit and error matrix are accepted.

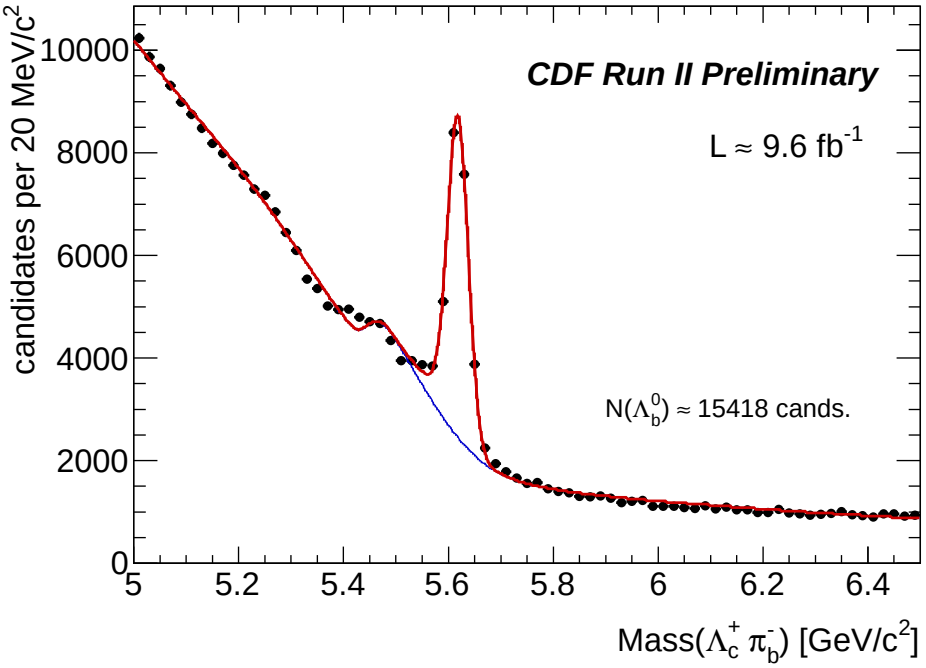

FIG. 1: Invariant mass distribution of $\Lambda_b^0 \to \Lambda_c^+\pi_b^-$ candidates with the projection of a mass fit overlaid.

TABLE III: Λ_b^{*0} candidate selection requirements.

Quantity	Requirement
$m(\Lambda_c^+\pi_b^-)$	$\in (5.561,\ 5.677)\,\mathrm{GeV}/c^2$
$d_0(\pi_s^\pm)$	< 0.1 cm
$p_\mathrm{T}(\pi_s^\pm)$	> 200 MeV/c
$d_0(\pi_s^\pm)/\sigma_{d_0}$	< 3.0

To reduce the background level, a kinematic fit is applied to the resulting combinations of Λ_b^0 candidate with two soft pion tracks $\pi_s^-\pi_s^+$ to constrain them to originate from a common point. Furthermore, since the bottom baryon resonance originates and decays at the primary vertex, the soft pion tracks are required to point back to the primary vertex by requiring an impact parameter significance $d_0(\pi_s^\pm)/\sigma_{d_0}$ smaller than 3. The Λ_b^{*0} candidate selection requirements are summarized in Table III.

IV. EXPERIMENTAL MASS DISTRIBUTION AND THE FIT

The analysis of the Λ_b^{*0} mass distributions is performed using the Q value

$$Q = m(\Lambda_b^0\pi_s^-\pi_s^+) - m(\Lambda_b^0) - 2\cdot m_\pi\ ,$$

where m_π is the known charged pion mass [34] and $m(\Lambda_b^0)$ is the reconstructed $\Lambda_c^+\pi_b^-$ mass. The mass resolution of the Λ_b^0 signal and most of the systematic uncertainties cancel in the mass difference spectrum. We search for the narrow structures in the Q value spectrum within a range of $6 - 50\,\mathrm{MeV}/c^2$.

The signal function is parametrized by two Gaussians taken with their widths $\sigma_{n,w}$ and weights g_n, $(1-g_n)$ according to Monte-Carlo simulation studies,

$$\mathcal{S}(Q;Q_0,\sigma_n,g_n,\sigma_w) \ = \ g_n\cdot\mathcal{G}_n(Q;Q_0,\sigma_n) \ + \ (1-g_n)\cdot\mathcal{G}_w(Q;Q_0,\sigma_w).$$

The dominant part of the signal function is a narrow core with a width σ_n of about $0.9\,\mathrm{MeV}/c^2$ and a relative weight g_n of about 70% while the wider tail portion has a width σ_w of about $2.3\,\mathrm{MeV}/c^2$. The background is described by the

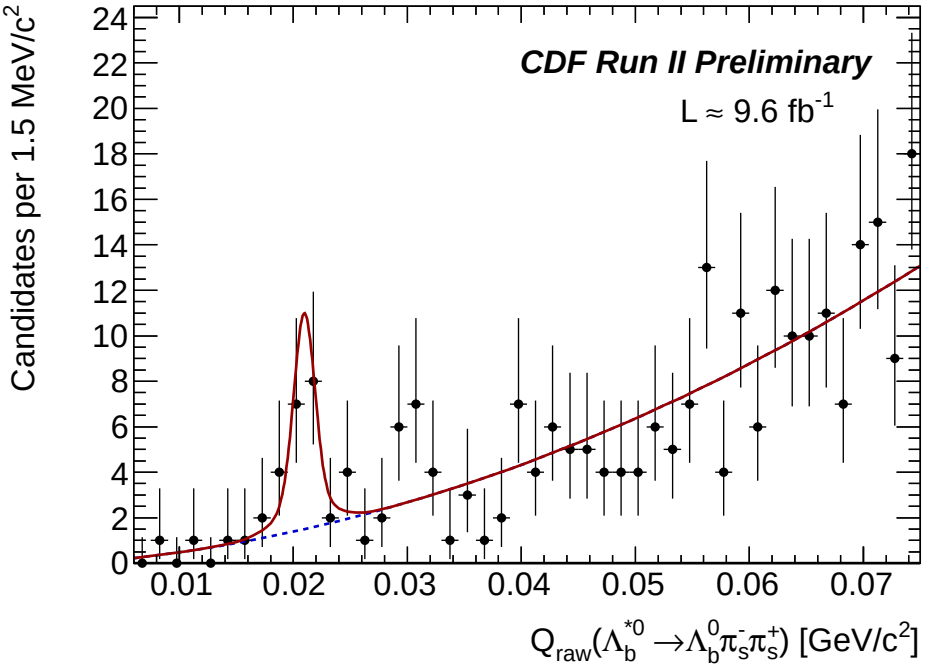

FIG. 2: The projection of the unbinned fit. The Q value for the Λ_b^{*0} candidates shown within $(0.006, 0.075)\,\mathrm{GeV}/c^2$. The soft pion tracks have a transverse momentum above $200\,\mathrm{MeV}/c$.

second order Chebyshev polynomial. The full model for the Q value spectra describes a single narrow structure on top of a smooth background. The parameters of interest are the position of the signal Q_0 and its yield, N candidates. The negative logarithm of the extended likelihood function (NLL) is minimized over the unbinned set of Q values observed for the candidates in our sample. The Q value spectrum is fit over the range $6 - 75\,\mathrm{MeV}/c^2$.

A. Soft pion momentum scale and Q value scale adjustment

We use our large sample of $D^{*+} \to D^0\pi_s^+$ events to calibrate the momentum scale of the soft pions. We find the Q value in D^{*+} decays to be $145.477\,\mathrm{MeV}/c^2$ which is by $0.056\,\mathrm{MeV}/c^2$ greater than the world-average value of $145.421\,\mathrm{MeV}/c^2$ [34]. In Monte Carlo simulations, we find that a scale factor of 0.99 applied to the the soft pion transverse momentum gives the observe mass shift. Using that scale factor of 0.99 for the soft pions in simulation of $\Lambda_b^{*0} \to \Lambda_b^0\pi_s^-\pi_s^+$ decays gives a mass shift of $-0.28\,\mathrm{MeV}/c^2$. We take the full value of the adjustment as the uncertainty and will apply a shift of -0.28 ± 0.28 MeV/c^2 to the Q value we find in a fit of the Λ_b^{*0} experimental spectrum.

B. Fit results

The experimental Λ_b^{*0} Q value distribution, fit with the unbinned likelihood described above, is shown in Fig. 2. The projection of the corresponding likelihood fit is superimposed on the graph. A narrow structure at $Q \sim 21\,\mathrm{MeV}/c^2$ is clearly seen. The fit finds $17.3^{+5.3}_{-4.6}$ signal candidates at $Q = 20.68 \pm 0.35$ MeV/c^2, where the resulting Q value is adjusted with the calibrated scale offset of $-0.28\,\mathrm{MeV}/c^2$.

C. Signal significance

The significance of the signals is determined using a log-likelihood ratio statistic [36, 37],

$$D \;=\; -2\,\ln(\mathcal{L}_0/\mathcal{L}_1) \;= -2\cdot\Delta(\log\mathcal{L})\,.$$

TABLE IV: Local significance of the observed signal against various null hypotheses. N_σ is the calculated number of Gaussian standard deviations based on Prob(χ^2).

Likelihood ratio	$-2\cdot\Delta(\log\mathcal{L})$	ΔNDF	Prob(χ^2)	N_σ
Values	$-2\cdot(-12.993)$	2	$\approx 2.276207\cdot 10^{-6}$	≈ 4.6

We define hypothesis $\mathcal{H}_1$ corresponding to the presence of Λ_b^{*0} signal on top of the background. The null $\mathcal{H}_0$ hypothesis is the background model described by the second order Chebyshev polynomial. The result is summarized in the Table IV. Our baseline signal fit has a local significance of ≈ 4.6.

The significance for a search window $Q \in (6.0, 50.0)\,\mathrm{MeV}/c^2$ has been determined running a number of statistical trials when $\mathcal{H}_0$ hypothesis is generated but fit with the $\mathcal{H}_1$ hypothesis and the corresponding log-likelihood ratio statistic is calculated per every trial. The fraction of the generated trials having $-\Delta(\log\mathcal{L})$ above the value returned by the fits of the experimental data, determines the significance. For this case the significance has been found to be $\approx 3.5\sigma$.

V. SYSTEMATIC UNCERTAINTIES

The systematic uncertainties considered in our analysis are the following:

(i) The uncertainty due to the CDF tracker momentum scale, dominating contribution.

(ii) The uncertainty due to the resolution model (see Sec. IV) described by the sum of two Gaussians.

(iii) The choice of background model.

To calibrate the tracker momentum scale, the energy loss in the material of CDF tracking detectors and the strength of the magnetic field must be determined. Both effects are calibrated and analyzed in detail using high statistics samples of J/ψ, $\psi(2S)$, $\Upsilon(1S)$, Z^0 reconstructed in their $\mu^+\mu^-$ decay modes as well as $D^0 \to K^-\pi^+$, $\psi(2S) \to J/\psi\,(\to \mu^+\mu^-)\pi^+\pi^-$ [38, 39]. The corresponding corrections are taken into account by tracking algorithms. Any systematic uncertainties on these corrections are largely negligible in the Λ_b^{*0} Q value measurements. The uncertainties on the measured mass differences due to the momentum scale of the low p_{T} $\pi_s^\pm$ tracks are estimated from the large statistics calibration D^{*+} sample, see Sec. IV A. The CDF Monte Carlo simulation typically underestimates the detector resolution what is considered as the source of a systematic uncertainty [21]. The statistical uncertainties on the resolution model parameters due to the finite size of the Monte Carlo datasets introduce another systematic uncertainty. Variations of the double Gaussian widths σ_n and σ_w and the weight g_n within their statistical uncertainties returned from the fits of Monte Carlo spectra are propagated into the measurable quantities. To find the systematic uncertainty associated with the choice of background shape, we change our background PDF to the 3-rd and 4-th power polynomials.

The uncertainties are summarized in the Table V.

VI. RESULTS AND CONCLUSIONS

The analysis results are arranged in Table VI. From the measured Λ_b^{*0} Q value we extract the absolute masses using the known value of the $\pi^\pm$ mass [34] and the CDF Λ_b^0 mass measurement, $m(\Lambda_b^0) = 5619.7 \pm 1.2\,(\mathrm{stat}) \pm 1.2\,(\mathrm{syst})\ \mathrm{MeV}/c^2$, as obtained in an independent sample [38]. The Λ_b^0 statistical and systematic uncertainties contribute to the systematic uncertainty on the Λ_b^{*0} absolute mass.

In conclusion, we have observed the $\Lambda_b^{*0} \to \Lambda_b^0\pi^-\pi^+$ resonance state in its Q value spectrum. The local significance of the signal is 4.6σ. The significance of the signal for the search region of $6-50$ MeV/c^2 is 3.5σ. Our result confirms the higher state $\Lambda_b^{*0}(5920)$ of the two recently observed by the LHCb Collaboration [22]. The result is consistent with recent theoretical predictions.

Acknowledgments

We thank the Fermilab staff and the technical staffs of the participating institutions for their vital contributions. This work was supported by the U.S. Department of Energy and National Science Foundation; the Italian Istituto

TABLE V: Summary of systematic uncertainties. The uncertainty due to the soft pion momentum scale is a dominating contribution.

Source	**Value**, MeV/c^2	**Comment**
Momentum scale	± 0.28	propagated from high statistics calibration D^{*+} sample; 100% of the found adjustment value.
Signal model	± 0.11	MC underestimates the resolution; choice of the model's parameters
MC resolution stat. uncertainty	± 0.012	finite MC sample size induces the stat. uncertainty of the shape parameters.
Background model	± 0.03	consider 3-rd, 4-th power polynomials
Total:	± 0.30	added in quadrature

TABLE VI: Summary of the final results. The first uncertainty is statistical and the second is systematic.

Value	MeV/c^2
Q	$20.68 \pm 0.35(\text{stat}) \pm 0.30(\text{syst})$
ΔM	$299.82 \pm 0.35(\text{stat}) \pm 0.30(\text{syst})$
$M(\Lambda_b^{*0})$	$5919.5 \pm 0.35\,(\text{stat}) \pm 1.72\,(\text{syst})$

Nazionale di Fisica Nucleare; the Ministry of Education, Culture, Sports, Science and Technology of Japan; the Natural Sciences and Engineering Research Council of Canada; the National Science Council of the Republic of China; the Swiss National Science Foundation; the A.P. Sloan Foundation; the Bundesministerium für Bildung und Forschung, Germany; the Korean World Class University Program, the National Research Foundation of Korea; the Science and Technology Facilities Council and the Royal Society, UK; the Russian Foundation for Basic Research; the Ministerio de Ciencia e Innovación, and Programa Consolider-Ingenio 2010, Spain; the Slovak R&D Agency; the Academy of Finland; and the Australian Research Council (ARC).

[1] M. Neubert, Phys. Rept. **245**, 259 (1994); A. V. Manohar and M. B. Wise, Camb. Monogr. Part. Phys. Nucl. Phys. Cosmol. **10**, 1 (2000).
[2] N. Isgur and M. B. Wise, Phys. Lett. B **232**, 113 (1989); *Ibid.* **237**, 527 (1990); N. Isgur and M. B. Wise, Phys. Rev. D **42**, 2388 (1990).
[3] J. G. Korner, M. Kramer, and D. Pirjol, Prog. Part. Nucl. Phys. **33**, 787 (1994).
[4] Throughout the text the notation Λ_b^{*0} represent $J^P = \frac{1}{2}^-$ or $J^P = \frac{3}{2}^-$ state.
[5] S. Capstick and N. Isgur, Phys. Rev. D **34**, 2809 (1986).
[6] M. Karliner, B. Keren-Zur, H. J. Lipkin, and J. L. Rosner, arXiv:0708.4027 [hep-ph]; M. Karliner, B. Keren-Zur, H. J. Lipkin, and J. L. Rosner, Annals Phys. **324**, 2 (2009); M. Karliner, Nucl. Phys. Proc. Suppl. **187**, 21 (2009).
[7] W. Roberts and M. Pervin, Int. J. Mod. Phys. A **23**, 2817 (2008).
[8] D. Ebert, R. N. Faustov, and V. O. Galkin, Phys. Rev. D **72**, 034026 (2005); D. Ebert, R. N. Faustov, and V. O. Galkin, Phys. Lett. B **659**, 612 (2008); D. Ebert, R. N. Faustov, and V. O. Galkin, Phys. Atom. Nucl. **72**, 178 (2009).
[9] E. E. Jenkins, Phys. Rev. D **54**, 4515 (1996); *Ibid.* **55**, R10 (1997); *Ibid.* **77**, 034012 (2008).
[10] Z. Aziza Baccouche, C. -K. Chow, T. D. Cohen and B. A. Gelman, Phys. Lett. B **514**, 346 (2001); Z. Aziza Baccouche, C. -K. Chow, T. D. Cohen and B. A. Gelman, Nucl. Phys. A **696**, 638 (2001).
[11] H. Garcilazo, J. Vijande, and A. Valcarce, J. Phys. G **34**, 961 (2007).
[12] J. R. Zhang and M. Q. Huang, Phys. Rev. D **78**, 094015 (2008); J. R. Zhang and M. Q. Huang, arXiv:0904.3391 [hep-ph].
[13] Y. Aoki *et al.* [RBC and UKQCD Collaborations], Phys. Rev. D **83**, 074508 (2011).

[14] R. Lewis and R. M. Woloshyn, Phys. Rev. D **79**, 014502 (2009).
[15] H. -W. Lin, S. D. Cohen, L. Liu, N. Mathur, K. Orginos and A. Walker-Loud, Comput. Phys. Commun. **182**, 24 (2011)
[16] W. Detmold, C. -J. D. Lin and S. Meinel, Phys. Rev. Lett. **108**, 172003 (2012)
[17] S. Capstick and W. Roberts, Prog. Part. Nucl. Phys. **45**, S241 (2000).
[18] X. H. Guo, K. W. Wei, and X. H. Wu, Phys. Rev. D **77**, 036003 (2008).
[19] C. W. Hwang, Eur. Phys. J. C **50**, 793 (2007).
[20] T. Aaltonen *et al.* (CDF Collaboration), Phys. Rev. Lett. **99**, 202001 (2007).
[21] T. Aaltonen *et al.* [CDF Collaboration], Phys. Rev. D **85**, 092011 (2012).
[22] RAaij *et al.* [LHCb Collaboration], arXiv:1205.3452 [hep-ex].
[23] D. Acosta *et al.* (CDF Collaboration), Phys. Rev. D **71**, 032001 (2005).
[24] A. Sill *et al.*, Nucl. Instrum. Meth. A **447**, 1 (2000); A. A. Affolder *et al.* (CDF Collaboration), Nucl. Instrum. Meth. A **453**, 84-88 (2000); S. Nahn (On behalf of the CDF Collaboration), Nucl. Instrum. Methods A **511**, 20 (2003); C. S. Hill (On behalf of the CDF Collaboration), Nucl. Instrum. Methods A **530**, 1 (2004).
[25] A. A. Affolder *et al.* (CDF Collaboration), Nucl. Instrum. Methods A **526**, 249 (2004).
[26] The CDF II detector uses a cylindrical coordinate system with z axis along the nominal proton beam line, radius r measured from the beam line and ϕ defined as an azimuthal angle. The transverse plane (r, ϕ) is perpendicular to the z axis. The polar angle θ is measured from the z axis. Transverse momentum $p_{\rm T}$ is the component of the particle's momentum projected onto the transverse plane. Pseudorapidity is defined as $\eta \equiv -\ln(\tan(\theta/2))$. The impact parameter of a charged particle track d_0 is defined as the distance of closest approach of the particle track to the primary vertex in the transverse plane.
[27] E. J. Thomson *et al.*, IEEE Trans. Nucl. Sci. **49**, 1063 (2002).
[28] B. Ashmanskas *et al.* (CDF Collaboration), Nucl. Instrum. Meth. A **518**, 532-536 (2004); L. Ristori and G. Punzi, Ann. Rev. Nucl. Part. Sci. **60**, 595-614 (2010).
[29] P. Nason, S. Dawson, and R. K. Ellis, Nucl. Phys. B **303**, 607 (1988); *Ibid.*, Nucl. Phys. B **327**, 49-92 (1989).
[30] C. Peterson, D. Schlatter, I. Schmitt, and P. M. Zerwas, Phys. Rev. D **27**, 105 (1983).
[31] D. J. Lange, Nucl. Instrum. Methods A **462**, 152 (2001).
[32] R. Brun, R. Hagelberg, M. Hansroul, and J.C. Lassalle, CERN Reports No. CERN-DD-78-2-REV and No. CERN-DD-78-2.
[33] Unless otherwise stated all references to a specific charge combination imply the charge conjugate combination as well. Specifically, $\overline{\Lambda}_b^{*0} \to \overline{\Lambda}_b^0 \pi_s^+ \pi_s^-$, $\overline{\Lambda}_b^0 \to \overline{\Lambda}_c^- \pi_b^+$, $\overline{\Lambda}_c^- \to \overline{p} K^+ \pi^-$, $D^{*-} \to \overline{D}^0 (\to K^+ \pi^-) \pi_s^-$.
[34] J. Beringer *et al.* (Particle Data Group), Phys. Rev. D **86**, 010001 (2012).
[35] A. Abulencia *et al.* (CDF Collaboration), Phys. Rev. Lett. **98**, 122002 (2007).
[36] S.S. Wilks, Ann. Math. Statist. **9** (1938) 60-2.
[37] R. Royall, J. Amer. Statist. Assoc. **95**, 760 (2000).
[38] D. Acosta *et al.* (CDF Collaboration), Phys. Rev. Lett. **96**, 202001 (2006).
[39] T. Aaltonen *et al.* (CDF Collaboration), Phys. Rev. Lett. **103**, 152001 (2009)